www.czasopisma.pan.pl PAN POLSKA AKADEMIA NAUK www.journals.pan.pl

Arch. Metall. Mater. **67** (2022), 3, 803-813

DOI: https://doi.org/10.24425/amm.2022.139670

J. ABUTHAKIR[1*], R. SUBRAMANIAN[1], K. SOMASUNDARA VINOTH[2], G. VENKATESH[1], G. SUGANYA PRIYADHARSHINI[3], K. KRISHNAKUMAR[1]

STUDIES ON MICROSTRUCTURAL EVOLUTION AND WEAR BEHAVIOUR OF AlNi INTERMETALLIC REINFORCED AA6061 ALLOY IN T6 CONDITION

In the present investigation Ni particles were added in varying weight fractions (0.5, 1.0 and 1.5%) to AA6061 alloy during stir casting. To prepare Al-Ni intermetallic reinforced Aluminium Metal Matrix Composites (Al MMCs), as-cast samples were subjected to T6 treatment (Solutionization at 550°C followed by ageing at 2,4,6,8 and 10 hours). Base alloy was also subjected to T6 treatment for comparison purpose. Hardness of the samples were obtained using Vickers hardness test. Samples in the peak aged (T6) condition were subjected to metallographic examination. Influence of Ni particles on the hardness and grain refinement was investigated. X-ray Diffraction analysis of the Ni added samples revealed the presence of Al-Ni intermetallic phase formation in the peak aged (T6) Condition. Scanning Electron Microscope – Energy Dispersive X-Ray Spectroscopy analysis of composites in the peak aged (T6) condition were carried out to study the formation of the Al-Ni intermetallic phase. Effect of Al-Ni intermetallic phase on wear and friction behavior of the composite samples were studied and compared with that of the base alloy in the peak aged (T6) condition.

Keywords: Al MMCs; Peak aged (T6) condition; Al-Ni intermetallic reinforced composites; Adhesive wear

1. Introduction

Intermetallic compounds reinforced Al Metal Matrix Composites (MMCs) are increasingly preferred over ceramic particles reinforced Al metal matrix composites due to their excellent interfacial bonding with the aluminium matrix coupled with enhanced high temperature stability. Thermal equilibrium between intermetallic compounds and aluminium matrix along with easy wettability of intermetallic compounds by molten aluminium leads to the strong interfacial bonding, resulting in better hardness and strengthening [1]. Owing to the special characteristics of intermetallic compounds, several studies have been carried out with intermetallic reinforcements such as AlNi, Al_3Ni, Al_3Ni_2, Al_3Ti and Al_2Cu [2]. Among these, nickel aluminide intermetallic compounds have been extensively investigated because of their low density and hard nature [3]. Nickel aluminide (AlNi, Al_3Ni and Al_3Ni_2) reinforced Al MMCs can be synthesized through stir casting, squeeze casting, Friction Stir Processing (FSP), Exo-melt process and solid state synthesis (mechanical alloying followed by T6 treatment). Synthesis of insitu intermetallics by using casting route/liquid state synthesis poses difficulties such as evaporation of lower melting point constituents and segragation in the microstructure [4,5]. Although FSP route can overcome this problems, several process parameters have to be optimized to achieve desired degree of intermetallic compound formation. Solid state synthesis route has been widely preferred as it can be applied to bulk synthesis. Several studies have reported synthesis of intermetallic compounds reinforced Al MMCs through Mechanical Alloying (MA) route [6]. Strong interfacial bonding can be achieved between matrix and intermetallic compounds through MA route. However, MA route involves optimization of several processing parameters such as milling time, milling speed, ball to powder ratio and atmosphere control to ensure good wettability and strong interfacial bonding between the matrix and intermetallic reinforcement [3]. These difficulties can be overcome by synthesis of intermetallic reinforced Al MMCs through T6 treatment of as-cast materials containing metallic particles.Naeem et al. [7] reported formation of nickel aluminide compounds through T6 treatment during their study on microstructural and mechanical behavior of Al-Zn-Mg-Cu

[1] METALLURGICAL ENGINEERING, PSG COLLEGE OF TECHNOLOGY, INDIA-641004
[2] PRODUCTION ENGINEERING, PSG COLLEGE OF TECHNOLOGY, INDIA-641004
[3] MECHANICAL ENGINEERING, COIMBATORE INSTITUTE OF TECHNOLOGY, INDIA-641004

* Corresponding author:thakir1988@gmail.com

alloy containing Ni and Sn particles. Farkoosh et al. [8] studied phase formation in Ni particles added Al-Si-Cu-Mg alloy in the heat treated condition. Numerous attempts have been made in the synthesis of nickel aluminide reinforced AA 6061 Al MMCs and ceramic particles reinforced Al MMCs through casting and FSP routes [9-12]. However, only a few studies in nickel aluminide reinforced Al MMCs synthesised through T6 treatment have been done, wherein comparable properties have been reported with those of FSP and MA routes [7,8,13,14]. Studies on nickel aluminide reinforced Al MMCs through various synthesis routes have shown improved tensile, impact, wear and corrosion properties of these materials compared to ceramic particle reinforced Al MMCs [3]. AA6061 alloy reinforced with nickel aluminide by FSP route have been widely investigated for their wear behavior [15].

In this study, AlNi intermetallic reinforced Al MMCs were synthesized through T6 treatment of as-cast samples, prepared through stir casting of AA6061 (Al-Si-Mg) alloy melt containing varying weight fractions (wt%) of Ni particles (0.5, 1.0 and 1.5%). Peak aged samples obtained in the T6 treatment were subjected to microstructural analysis, hardness and grain size measurement. X-ray diffraction (XRD), Scanning Electron Microscope – Energy Dispersive X-Ray Spectroscopy (SEM – EDAX) was carried out on composites in the peak aged (T6) condition to study intermetallic phase formation. Wear studies of peak aged samples were carried out to find the influence of AlNi intermetallic reinforcement on the wear rate and friction coefficient using an L9 orthogonal array.

2. Materials and experimental work

AA6061 alloy was melted in a furnace maintained at a temperature of 750°C. Ni particles preheated at 200°C were added to the melt and mixture was stirred for 10 minutes at 200 rpm. Ni particles with average size of 50 µm and spherical morphology was used in the current investigation (Fig. 1). Weight fractions of Ni particles used in the investigation was 0.5, 1.0 and 1.5%. Chemical composition of base alloy and composite samples (TABLE 1) was obtained using Optical Emission Spectroscopy (OES – BRUKER).

TABLE 1

Chemical composition (weight %) of base alloy and composite samples in the as-cast condition

	Ni	Si	Mg	Fe	Cu	Mn	Al
Base alloy	—	0.77	0.85	0.415	0.279	0.082	Remainder
AA6061 + 0.5 Wt% Ni composite	0.5	0.613	0.761	0.190	0.229	0.074	Remainder
AA6061 + 1.0 Wt% Ni composite	1.0	0.598	0.735	0.188	0.221	0.0720	Remainder
AA6061 + 1.5 Wt% Ni composite	1.5	0.565	0.715	0.183	0.215	0.0715	Remainder

As-cast samples were solutionized at 550°C followed by ageing at 165°C for 2, 4, 6, 8 and 10 hours to form AlNi intermetallic phase as reinforcement in the AA6061 alloy. Vickers hardness of as-cast and T6 treated samples was obtained using a 100g load. Samples with maximum hardness (peak aged samples) observed in the hardness survey were considered for further studies. Optical microscopy was carried out for composites in as-cast and peak aged (T6) condition. Samples were etched with 10% HF solution for optical microscopic examination. Grain size of the samples were measured using linear intercept method. Phase analysis using SEM-EDAX (TEAM) and XRD (SHIMADZU) were carried out for peak aged samples (base alloy and composite). X-ray Diffraction studies with Cu-Kα (1.54A°) radiation was carried out with a scanning range of 5°-90°, in steps of 0.0530° and a scan step time of 1second. Wear studies on the base alloy and composites were done using a DUCOM pin-on-disc wear tester as per ASTM G99 standard. Counter pin material used in the wear test was E11 hardened steel disc. Design of Experiments methodology with a three level fractional factorial design was used (L9 array) for conducting wear experiments (TABLE 2).

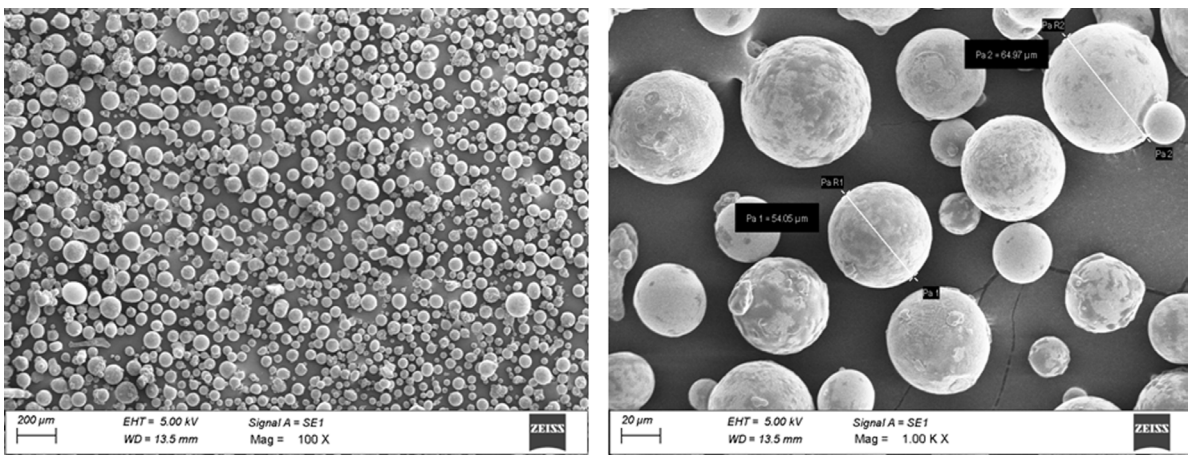

Fig. 1. SEM micrograph of Ni particles used in the investigation

TABLE 2

Levels of parameters used in L9 orthogonal array

Levels of factors	Ni (weight fraction)	Load (N)	Sliding speed (m/s)
1	0.5	10	1
2	1.0	20	2
3	1.5	30	3

Parameters used in the investigation were weight fraction (wt%) of Ni particles (0.5, 1.0 and 1.5%), sliding speed (1, 2 and 3 m/s) and load (10, 20 and 30 N). Sliding distance was fixed at 500 m and responses studied were wear rate and Coefficient of Friction (CoF) of the composites. Base alloy was tested using parameters corresponding to best and worst wear results obtained for composites. Wear and friction results were analysed using mean of wear loss/Coefficient of Friction (CoF), mean of S/N ratio and Analysis of Variance (ANOVA). Wear morphologies of all the wear samples were investigated using SEM (ZEISS).

3. Results and discussions

3.1. Hardness and microstructure of samples in the peak aged (T6) condition

Vickers hardness of the samples in the as-cast condition (TABLE 3) indicated an increase with increasing Ni weight percentage. Hardness of the samples subjected to T6 treatment at various ageing times (TABLE 4a) and in peak aged (T6) condition (TABLE 4b) revealed that base alloy attained peak hardness after 8 hours of ageing while composite samples attained peak hardness after 4 hours of ageing. Composites exhibited higher hardness than base alloy in T6 (TABLE 4b) and as-cast conditions (TABLE 3). Composites also showed higher hardness in T6 condition (TABLE 4b) compared to as – cast samples (TABLE 3). AA6061 + 1.5 Wt% Ni composite attained an increase of 30% in hardness from that of the base alloy in T6 condition. Jinwan Qian et al. [16] have reported a similar increase in hardness (97 VHN) in Al_3Ni reinforced Al alloy.

TABLE 3

Hardness of the as-cast samples

	Base alloy	AA6061 + 0.5 Wt% Ni composite	AA6061 + 1.0 Wt% Ni composite	AA6061 + 1.5 Wt% Ni composite
VHN	93	110	115	118

TABLE 4A

Hardness of the samples subjected to T6 treatment at various ageing times

Hardness scale	VHN			
Ageing time/ hardness	Base alloy	AA6061 + 0.5 Wt% Ni composite	AA6061 + 1.0 Wt% Ni composite	AA6061 + 1.5 Wt% Ni composite
2 Hours	89	93	104	137
4 Hours	91	128	140	153
6 Hours	113	113	120	126
8 Hours	117	110	117	108
10 Hours	106	103	107	103

TABLE 4B

Hardness of the samples in peak aged (T6) condition

Hardness	Base alloy	AA6061 + 0.5 Wt% Ni composite	AA6061 + 1.0 Wt% Ni composite	AA6061 + 1.5 Wt% Ni composite
VHN	117	128	140	153
% increase in hardness from that of the base alloy	—	9.4%	20%	30%

Optical micrographs of (Figs 2 and 3) the samples, revealed α-phase and eutectic grain boundary structure in both as-cast and T6 Conditions. Extent of grain refinement increases with increase in nickel percentage for both the conditions. Grain refinement of the samples in peak aged (T6) condition was higher than in as-cast condition due to dissolution of Ni particles at the grain boundary (Fig. 3).

TABLE 5

Grain size of the base alloy and composite samples in the peak aged (T6) condition

Samples	Grain size (micron)	Percentage change in grain size
Base alloy	64	—
AA6061 + 0.5 Wt% Ni composite	54	15%
AA6061 + 1.0 Wt% Ni composite	50	21%
AA6061 + 1.5 Wt% Ni composite	38.4	40%

The overall grain size reduction (TABLE 5) for AA6061 + 1.5 Wt% Ni composite was found to be 40% (T6 Condition) compared to the base alloy (Fig. 3). Increase in grain refinement can be clearly observed with increase in nickel weight percentage (Fig. 3) and can be attributed to the increased number of heterogeneous nucleation sites provided by the nickel particles. Gbenebor et. al [17] and Nadella et al. [18] have observed a similar increase in grain refinement in the case of Al alloys reinforced with particles. However AA6061 + 1.0 Wt% Ni composite exhibited only a marginal increase in grain refinement compared to AA6061 + 0.5 Wt% Ni composite

3.2. XRD investigations on alloy and composites in the peak aged (T6) condition

The phases present in the base alloy and composite samples in the peak aged (T6) condition is shown in the XRD pattern

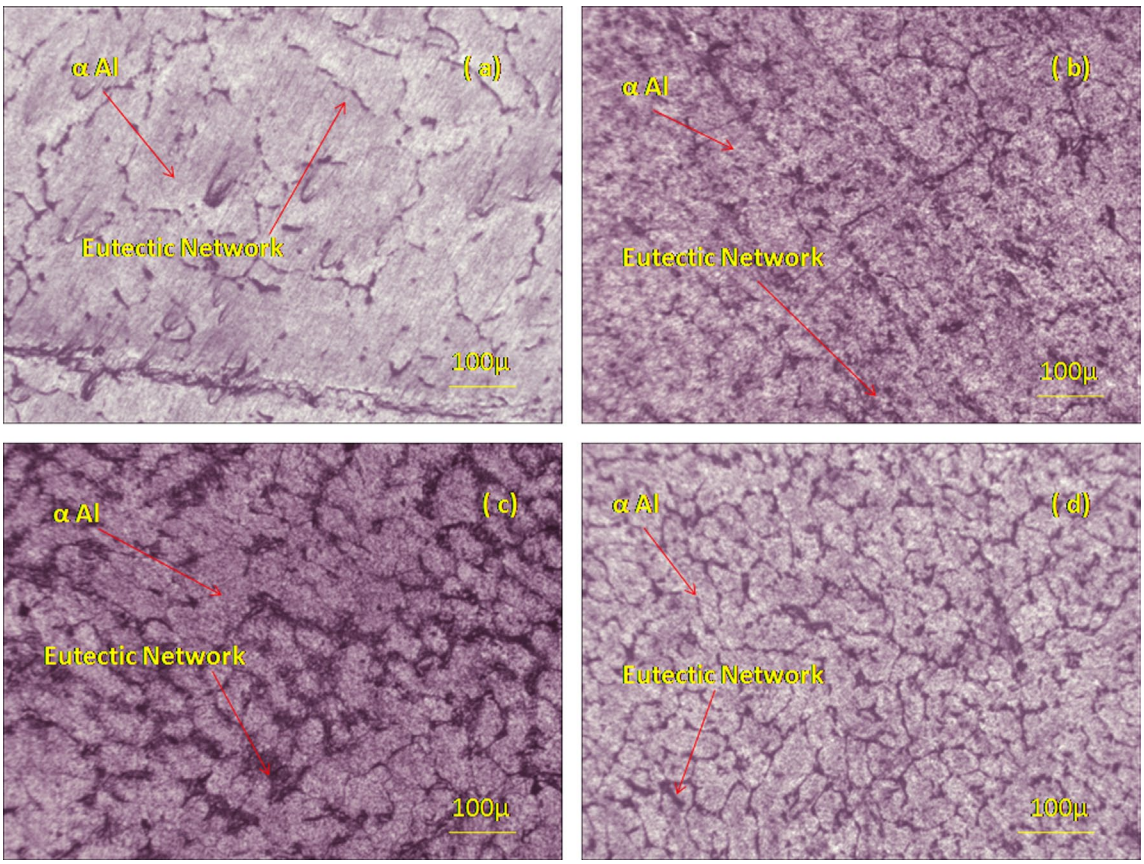

Fig. 2. Optical micrograph of (a) Base alloy (b) AA6061 + 0.5 Wt% Ni composite (c) AA6061 + 1.0 Wt% Ni composite and (d) AA6061 + 1.5 wt% Ni composite in the as-cast condition

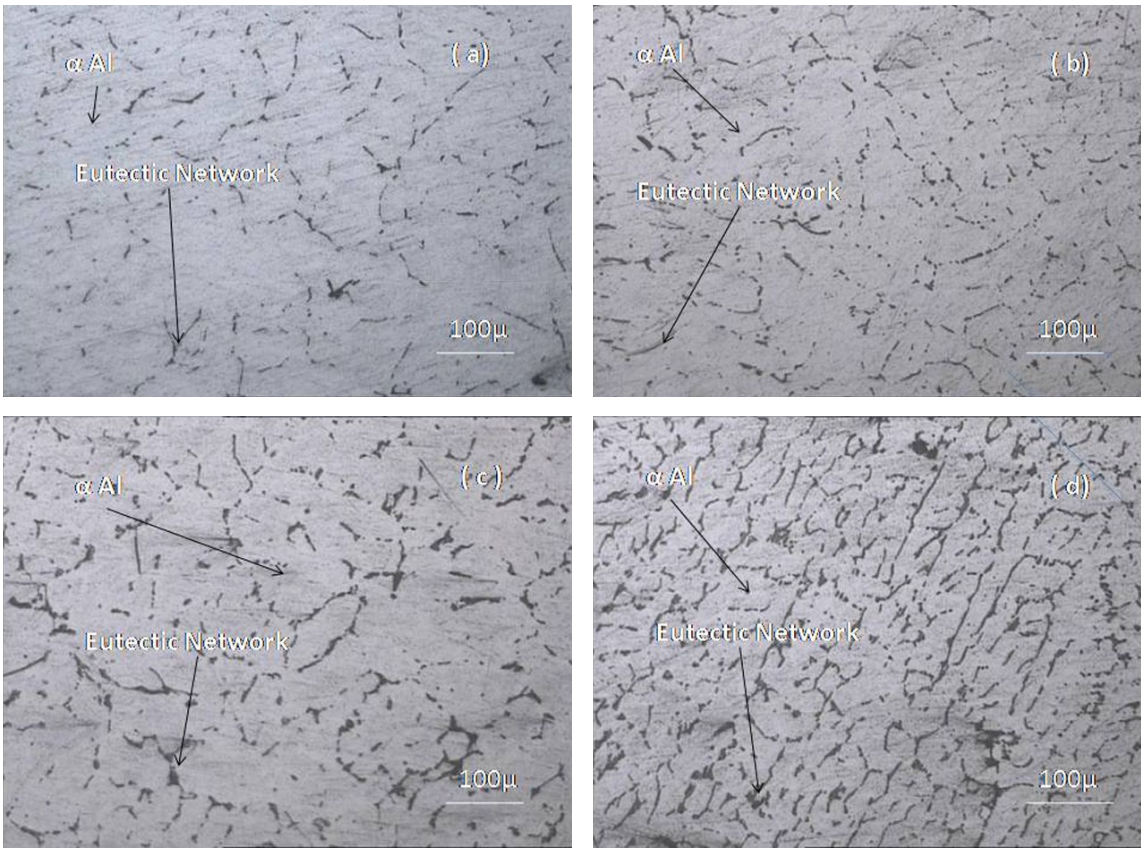

Fig. 3. Optical micrograph of (a) Base alloy (b) AA6061 + 0.5 Wt% Ni composite (c) AA6061 + 1.0 Wt% Ni composite and (d) AA6061 + 1.5 wt% composite in the peak aged (T6) Condition

(Fig. 4). Base alloy showed peaks of Al (ICDD pdf card no: 00-001-1176) and $Al_{3.2}Si_{0.47}$ (ICDD pdf card no: 00-041-1222) peaks at 2θ values of 38.3°, 65.1°, 78.2° and 82.3°, while AlMg peak (ICDD pdf card no: 00-042-1074) was observed at a 2θ value of 44.3°. XRD pattern of AA6061 + 0.5 Wt% Ni composite sample revealed that the peak obtained at 2θ value of 44.3° is higher in intensity than the base alloy. This indicated the presence of AlNi (ICDD pdf card no: 00-044-1186) intermetallic phase formation along with AlMg. AA6061 + 0.5 Wt% Ni composite also showed peaks of Al and $Al_{3.2}Si_{0.47}$ at 2θ values of 38.3°, 65.1°, 78.2° and 82.3°. AA6061 + 1.0 Wt% Ni composite revealed a high intensity peak at 2θ value of 44.3° compared to AA6061 + 0.5 Wt% Ni composite due to increased addition of Ni particles. Peak of AA6061 + 1.0 Wt% Ni composite at 2θ value of 44.3° corresponds to AlNi and AlMg. Peaks of AA6061 + 1.0 Wt% Ni composite at 2θ values of 38.3°, 65.1°, 78.2° and 82.3° were found to be Al and $Al_{3.2}Si_{0.47}$. XRD results of AA6061 + 1.5 Wt% Ni composite indicated that peak at 2θ value of 44.3° was much intense (1, 00,000 counts) than the other composite samples and it can be concluded that more amount of AlNi phase formation has taken place than other composites. In AA6061 + 1.5 Wt% Ni composite, AlNi and AlMg phases were found at 2θ values of 44.3°. Al and $Al_{3.2}Si_{0.47}$ phases were found at 2θ values of 38.3° and 82.3°. The values of d-spacing and planes obtained for the base alloy and composite samples are shown below (TABLE 6).

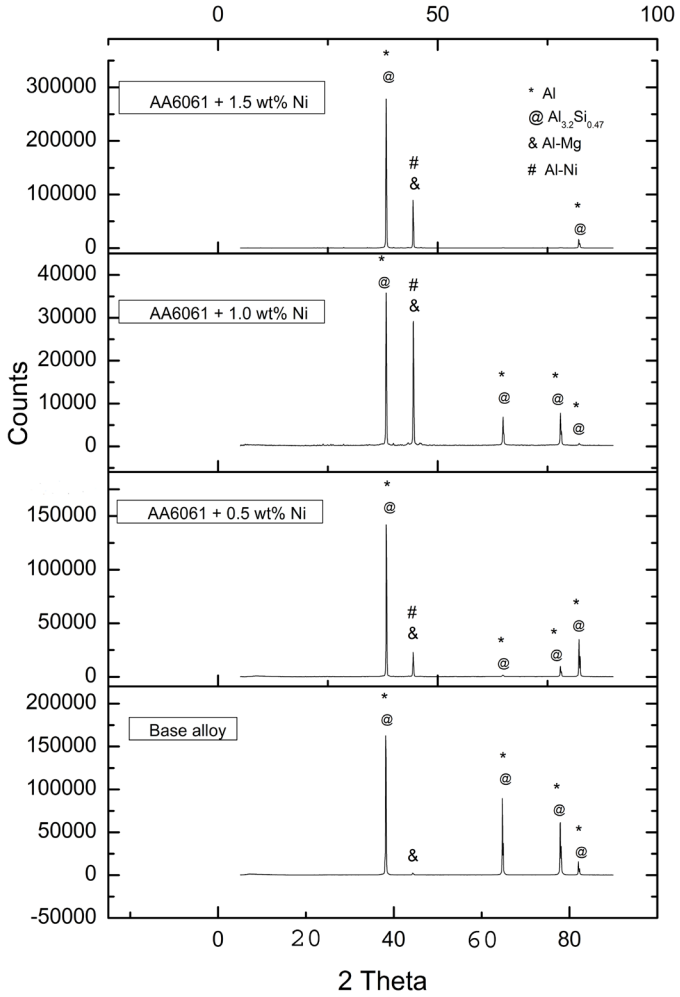

Fig. 4. Summary of XRD results of base alloy and composite samples in the peak aged (T6) condition

TABLE 6

Plane and d-spacing values of samples in the peak aged (T6) condition

	2θ value	Phases formed	d-spacing (A°)	Planes
Base alloy	38.3	$Al/Al_{3.2}Si_{0.47}$	2.34	(111)
	44.3	Al-Mg	2.03	(422)
	65.1	$Al/Al_{3.2}Si_{0.47}$	1.43	(220)
	78.2	$Al/Al_{3.2}Si_{0.47}$	1.22	(311)
	82.3	$Al/Al_{3.2}Si_{0.47}$	1.17	(222)
AA6061 + 0.5 Wt% Ni composite	38.3	$Al/Al_{3.2}Si_{0.47}$	2.34	(111)
	44.3	Al-Mg/Al-Ni	2.03	(422)/(110)
	65.1	$Al/Al_{3.2}Si_{0.47}$	1.43	(220)
	78.2	$Al/Al_{3.2}Si_{0.47}$	1.22	(311)
	82.3	$Al/Al_{3.2}Si_{0.47}$	1.17	(222)
AA6061 + 1.0 Wt% Ni composite	38.3	$Al/Al_{3.2}Si_{0.47}$	2.34	(111)
	44.3	Al-Mg/Al-Ni	2.03	(422)/(110)
	65.1	$Al/Al_{3.2}Si_{0.47}$	1.43	(220)
	78.2	$Al/Al_{3.2}Si_{0.47}$	1.22	(311)
	82.3	$Al/Al_{3.2}Si_{0.47}$	1.17	(222)
AA6061 + 1.5 Wt% Ni composite	38.3	$Al/Al_{3.2}Si_{0.47}$	2.34	(111)
	44.3	Al-Mg/Al-Ni	2.03	(422)/(110)
	65.1	—	—	—
	78.2	—	—	—
	82.3	$Al/Al_{3.2}Si_{0.47}$	1.17	(222)

It can be further seen that in the case of AA6061 + 0.5 Wt% Ni composite, the diffusion was limited due to lower weight fraction of Ni as seen from the XRD peaks (Fig. 4). However, with increasing weight fractions of Ni particles (1.0 and 1.5%), enhanced diffusion occurred due to large number of activation sites. Naeem et al. [7] reported formation of highly intense AlNi peaks during their studies on Ni/Sn additions to Al-Zn-Mg-Cu alloy and attributed them to the dissolution of Ni in the matrix brought by T6 treatment. In the present study, AA6061 + 1.5 Wt% Ni composite showed highest intensity peak at 2θ value of 44.3° confirming the formation of increased amount of AlNi phase (Fig. 4). Similar results have been reported in AlNi intermetallics reinforced Al MMCs. Guang Li et al. [19] reported formation of such peaks during investigations on AA 6061 Al MMCs reinforced with Ni decorated graphene particles. Reddy et al. [20] reported Al peaks during their studies on insitu Al_3Ni/Al_2O_3 reinforced Al hybrid matrix composites. Ali Reza Najarian et al. [21] and R. Ramesh et al. [22] have reported similar peaks for Al. T. Satish Kumar et al. [23] reported similar peaks for Al phase in zircon reinforced Al alloy. AlNi peak as reported in the current investigation was also observed by Kahtan s. Mohammad et al. [3]. Higher hardness (TABLE 4b) and grain refinement (Fig. 3d) of AA6061 + 1.5 Wt% Ni composite can be correlated with increasing amount of AlNi formation.

3.3. SEM-EDAX analysis of base alloy and composites in the peak aged (T6) condition

EDAX analysis of base alloy (Fig. 5a) revealed the presence of Mg and Si, both within the grains and eutectic network in the Al matrix. The results are in confirmation with XRD pattern of base alloy (Fig. 4). AA6061 + 0.5 Wt% Ni composite showed the presence of AlNi intermetallic phase in the eutectic network (Fig. 5b). The presence of relatively higher amount of AlNi intermetallic phase can be observed in the AA6061 + 1.0 Wt% Ni composite (Fig. 5c). AA6061 + 1.5 Wt% Ni composite revealed the presence of higher amount of AlNi intermetallic phase along the eutectic network (Fig. 5d). The increase in amount of the AlNi intermetallic phase in composite samples with increasing weight fraction of Ni particles, can also be seen from XRD results (Fig. 4) with a most intense AlNi peak for AA6061 + 1.5 Wt% Ni composite, indicating that XRD and EDAX results are in agreement with one another.

EDAX analysis of composite samples revealed that AlNi intermetallic phase have been formed in AA6061 grains and as well as in grain boundary network. Amount of AlNi intermetallic reinforcement increased with an increase in weight fraction of Ni particles due to increase in solid state reaction between the Ni particles and the AA6061 matrix in the heterogenous nucleation sites [17,18] thus resulted in dissolution of Ni particles. This resulted in increase in hardness (TABLE 4b) and grain refinement (TABLE 5). Similar observations have been reported in the AlNi intermetallic reinforced Al MMCs [1].

3.4. Wear of base alloy and composites in the peak aged (T6) condition

3.4.1. Statistical analysis

Wear loss and co-efficient of friction of composite samples in peak aged (T6) condition have been recorded during the wear test (TABLE 7). Main effects plot for mean of wear loss (Fig. 6a) showed that the wear loss decreased with an increase in the weight fraction of Ni. However, the wear loss increased with an increase

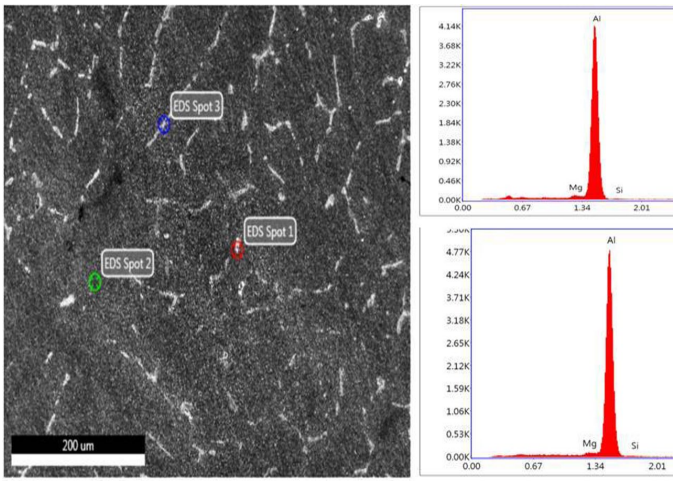

Fig. 5a. EDAX (spot) analysis of Base alloy in the peak aged (T6) condition

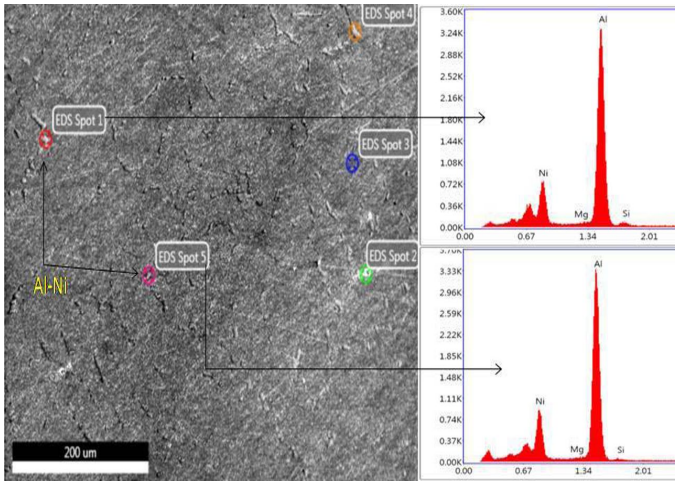

Fig. 5b. EDAX (spot) analysis of AA6061 + 0.5 Wt% Ni composite in the peak aged (T6) condition

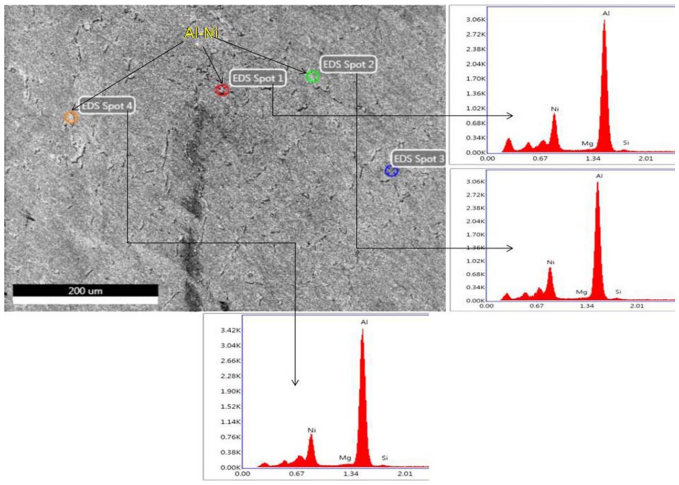

Fig. 5c. EDAX (spot) analysis of AA6061 + 1.0 Wt% Ni composite in the peak aged (T6) condition

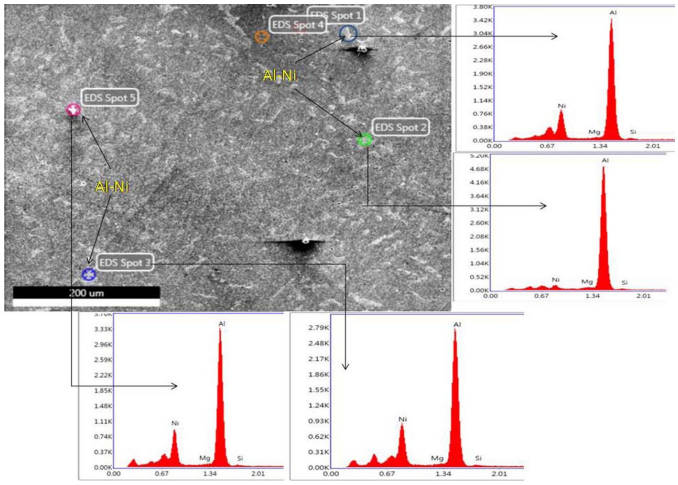

Fig. 5d. EDAX (spot) analysis of AA6061 + 1.5 Wt% Ni composite in the peak aged (T6) condition

in the load and sliding speed. Main effects plot for mean of S/N ratio (smaller the better characteristics) (Fig. 6b) is in agreement with main effects plot for mean of wear loss (Fig. 6a). Response table for mean of wear loss (TABLE 8) indicated that sliding speed influenced the wear of composites more than other factors (load and Ni weight fraction). However it can also be observed (TABLE 8) that the weight fraction of Ni particles also influenced the wear of composites and the applied load showed the least influence on the wear of the composites. Wear loss of AA6061 + 1.5 Wt% Ni composite is relatively lower than wear of other composites at all levels of sliding speed and load. This can be attributed to higher amount of AlNi intermetallic phase formed in AA6061 + 1.5 Wt% Ni composite (Fig. 5d) which resulted in grain refinement and higher hardness. AA6061 + 1.0 Wt% Ni composite had exhibited lower wear loss than AA6061 + 0.5 Wt% Ni composite for all levels of sliding speed and load owing to relatively higher fraction of AlNi intermetallic phase formed than in the AA6061 + 0.5 Wt% Ni composite. Wear loss of base alloy at tested conditions (TABLE 9) was comparable with that of AA6061 + 0.5 Wt% Ni composite. It can be revealed that difference in wear loss between successive levels of load was almost equal (Fig. 6a). It can also be concluded (Fig. 6a) that difference in wear loss between successive levels of sliding speed is not equal. Intermetallic reinforced Al MMCs have found to give better wear resistance as reported in various studies. Ramesh et al. [22] reported that AlNi reinforced AA1100 Al alloy shown better wear resistance compared to that of AA1100 alloy due to increase in hardness imparted by AlNi reinforcements. Srinivasan et al. [24] during investigations on the wear resistance of Ni coated CNT reinforced AA6061 alloy found that wear resistance improved due to better bonding exhibited by Ni coating over large surface area with AA6061 alloy. Zadali et al. [25] observed that aluminide reinforced Al alloy exhibited improved hardness and wear resistance.

TABLE 7

Wear experiment results of samples in the peak aged (T6) condition

Trial	Composition (%Ni)	Load (N)	Speed (m/s)	Wear (microns)	Coefficient of friction
1	0.5	10	1	26.68	0.912
2	0.5	20	2	224.35	0.681
3	0.5	30	3	544.16	0.582
4	1.0	10	2	21.85	0.957
5	1.0	20	3	147.63	0.723
6	1.0	30	1	83.93	0.826
7	1.5	10	3	121.18	0.764
8	1.5	20	1	17.53	0.960
9	1.5	30	2	19.04	0.948

TABLE 8

Response table for mean of wear loss of composite samples in the peak aged (T6) condition

Level	Ni (Weight fraction)	Load (N)	Sliding speed (m/s)
1	265.06	56.57	42.71
2	84.47	129.84	88.41
3	52.8	215.71	270.99
Delta	212.48	159.14	228.28
Rank	2	3	1

TABLE 9

Wear results of base alloy in the peak aged (T6) condition

Trial	Load (N)	Speed (m/s)	Wear (microns)	Coefficient of friction
1	20	1	51.5	0.887
2	30	3	604.48	0.476

3.4.2. Morphology of worn-out surface of base alloy and composites in the peak aged (T6) condition

Wear morphologies of AA6061 + 0.5 Wt% Ni composite shows mild adhesive wear features such as wear track, grooves and debris at a sliding speed of 1 m/s and a load of 10 N (Fig. 8a). At a sliding speed of 2m/s and load of 20 N, specimen revealed delamination and grooves (Fig. 8b) indicating a transition from mild to moderate adhesive wear mechanism**.** AA6061 + 0.5 Wt% Ni composite at a sliding speed of 3 m/s experienced severe delamination (Fig. 8c). AA6061 + 1.0 Wt% Ni composite had undergone relatively a lesser degree of severe delamination than AA6061 + 0.5 Wt% Ni (Fig. 8e) at a sliding speed of 3 m/s and applied load of 20N. AA6061 + 1.0 Wt% Ni composite also

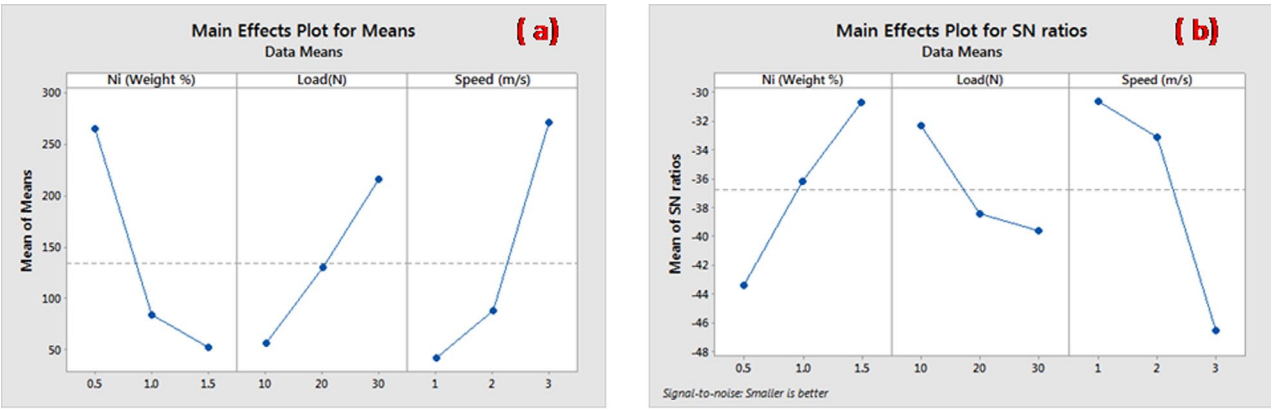

Fig. 6. Main effects plot for (a) mean of wear loss (b) mean of S/N ratio of the composite samples in the peak aged (T6) condition

shows presence of wear track and debris at sliding speeds of 2m/s and 1m/s (Fig. 8d-f). AA6061 + 1.0 Wt% Ni composite also shows mild delamination at sliding speed of 2m/s and 10 N (Fig. 8d). Both AA6061 + 0.5 Wt% Ni composite and AA6061 + 1.0 Wt% Ni composite had undergone severe delamination at sliding speed of 3m/s irrespective of the load conditions, indicating the influence of sliding speed. However AA6061 + 1.0 Wt% Ni composite had showed only few wear tracks compared to AA6061 + 0.5 Wt% Ni composite. This improvement in wear resistance can be attributed to enhanced hardness (TABLE 4b) which resulted from both grain refinement and as well as higher volume fraction of AlNi intermetallic reinforcements formed by increased Ni addition (Fig. 4).Wear micrographs (Fig. 7) shows that at sliding speed of 1m/s and 20 N, base alloy was revealed

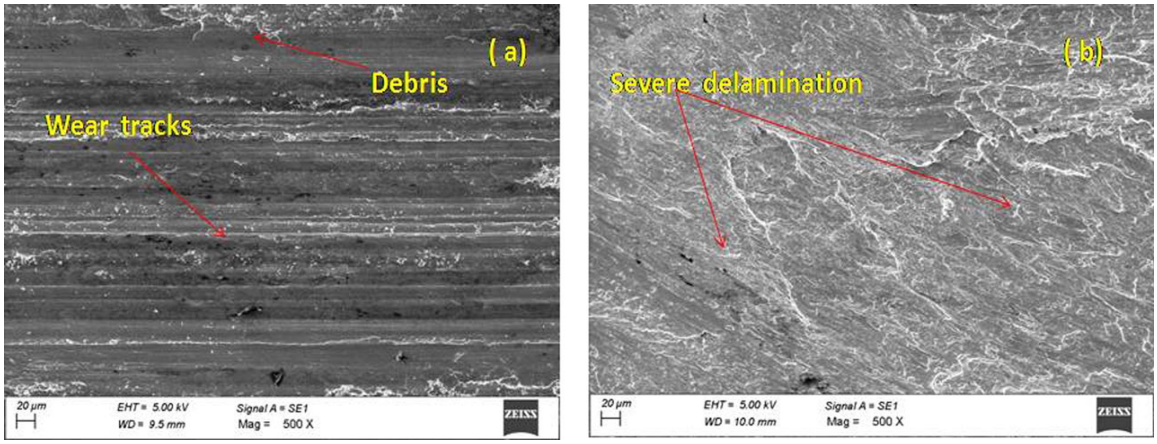

Fig. 7. Wear morphology of base alloy in the peak aged (T6) condition at (a) 20 N and 1 m/s (b) 30 N and 3 m/s

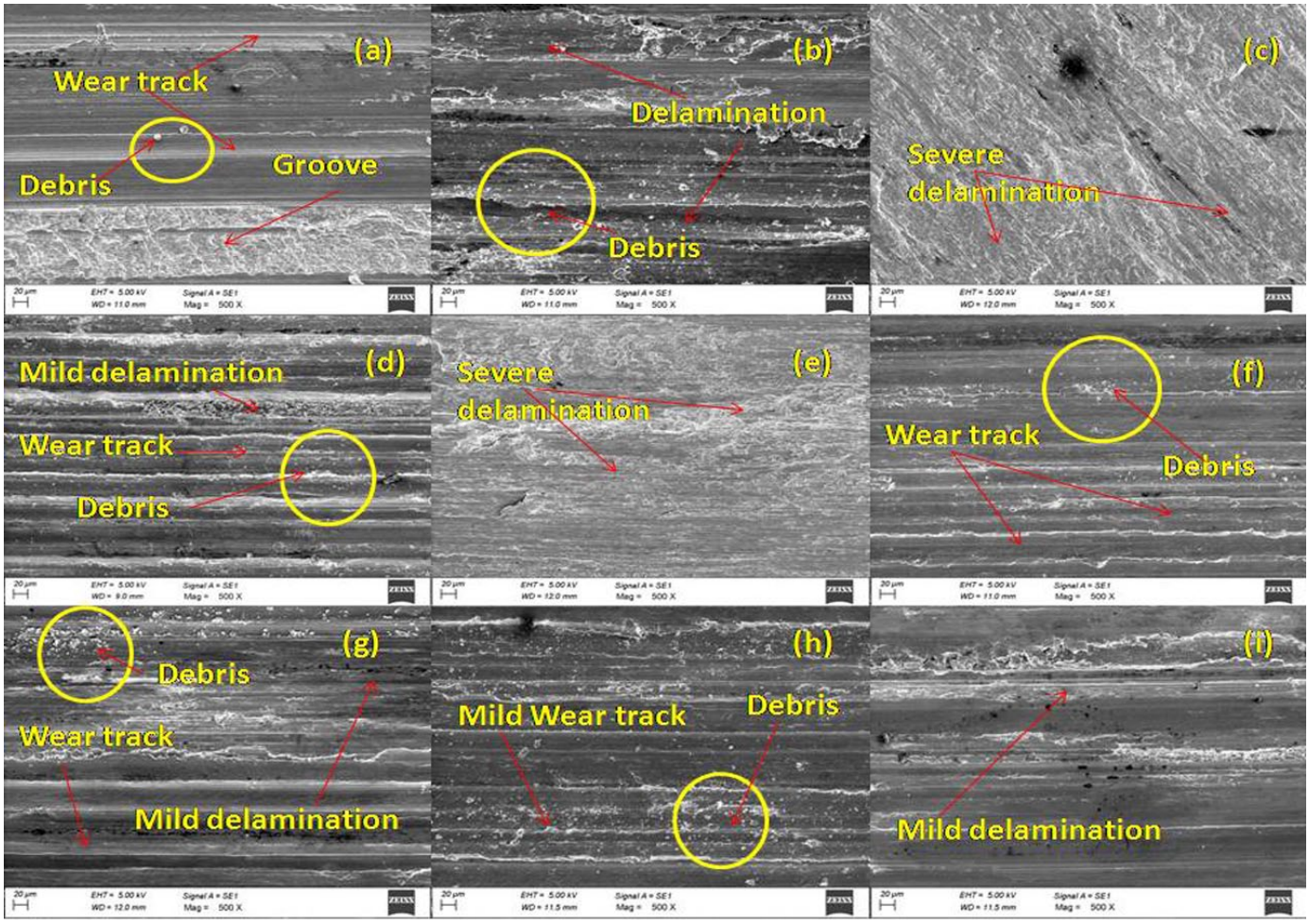

Fig. 8. Wear micrograph of composite samples in the peak aged (T6) condition; AA6061 + 0.5 Wt% Ni composite (a) 10 N and 1 m/s (b) 20 N and 2 m/s (c) 30 N and 3 m/s; AA6061 + 1.0 Wt% Ni composite (d) 10 N and 2 m/s (e) 20 N and 3 m/s (f) 30 N and 1 m/s; AA6061 + 1.5 Wt% Ni composite (g) 10 N and 3 m/s (h) 20 N and 1 m/s (i) 30 N and 2 m/s

with large number of wear tracks, debris and delamination. This behavior is quite comparable with the AA6061 + 0.5 Wt% Ni composite at lower sliding speed of 1m/s but relatively poor than AA6061 + 1.0 Wt% Ni composite. At sliding speed of 3m/s the base alloy also had undergone severe delamination (Fig. 7b).

AA6061 + 1.5 Wt% Ni composite showed fewer wear tracks and debris for all test conditions (Figs 8g-i). However, at a sliding speed of 3 m/s and a load of 10N, AA6061 + 1.5 Wt% Ni composite exhibited mild delamination and this shows the influence of sliding speed on the wear behaviour. On a comparative basis, AA6061 + 1.5 wt% composite showed lower wear loss than other composites due to higher fraction of AlNi intermetallic phase present.

In summary, all the composite samples exhibited adhesive wear with typical delamination, wear track and debris. It can also be said that severe delamination has occurred in the AA6061 + 0.5 Wt% Ni composite and AA6061 + 1.0 Wt% Ni composite, whereas AA6061 + 1.5 Wt% Ni composite had undergone mild delamination even at sliding speed of 3 m/s. This indicates that AA6061 + 1.5 Wt% Ni composite has shown better wear resistance than other composites and the base alloy in the peak aged (T6) condition. Radhika et al. [26] carried out wear investigation on age hardened AA6061Al hybrid MMCs and reported severe delaminations only at higher sliding speeds of 3 m/s and 4 m/s.

3.4.3. Co-efficient of Friction (CoF) of composites and base alloy in peak aged (T6) condition

Wear tests revealed that CoF of all the composite samples (TABLE 7) at a sliding speed of 3m/s was relatively lower than the CoF values at sliding speeds of 1 m/s and 2 m/s for all test conditions. Base alloy also exhibited a similar trend with respect to CoF (TABLE 9). Response table (TABLE 10) for mean of CoF values indicated that sliding speed exhibited a higher influence in affecting CoF of the composite samples followed by weight fraction of Ni particles and load.

CoF increases with increase in weight fraction of Ni particles whereas it decreases with increase in load and sliding speed for all the tested conditions (Fig. 9a). Main effects plot for mean of S/N ratio (Fig. 9b) also revealed that with increase in Ni weight fraction CoF of the composite samples increased but decreased with an increase in both load and sliding speed. It can be said that AA6061 + 1.5 Wt% Ni composite exhibited the highest COF for all test conditions compared to the other composites.

TABLE 10

Response table for mean of CoF of composites in the peak aged (T6) condition

Level	Ni (Weight fraction)	Load (N)	Sliding speed (m/s)
1	0.725	0.879	0.899
2	0.836	0.788	0.863
3	0.890	0.785	0.687
Delta	0.165	0.093	0.207
Rank	2	3	1

4. Conclusions

In the present investigation AlNi intermetallic reinforced Al MMCs were synthesized by T6 treatment of AA6061 alloy containing varying weight fraction of nickel particles (0.5, 1.0 and 1.5%). Major conclusions from the investigations are:

1. Hardness of composites in the peak aged (T6) and as-cast conditions increased with an increase in weight fraction of Ni particles. AA6061 + 1.5 Wt% Ni composite showed highest hardness and more effective grain refinement than other composites and base alloy under both as-cast and peak aged (T6) conditions.
2. Optical microstructure of samples in both the conditions showed increasing degree of grain refinement with an increase in weight fraction of Ni particles. Grain refinement of samples in the peak aged (T6) condition was better than the as-cast samples due to dissolution of Ni particles and thus resulting in higher hardness of the samples in the peak aged (T6) condition
3. XRD analysis of composite in the peak aged (T6) condition revealed the formation of AlNi intermetallic phase (reinforcement). It was also observed that the amount of

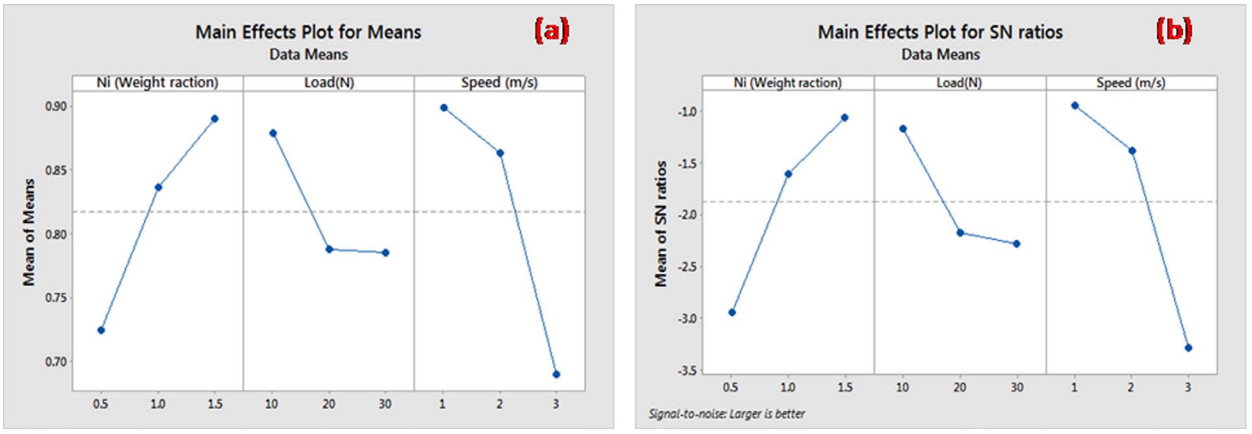

Fig. 9. Main effects plot for (a) mean of CoF (b) mean of S/N ratio of the composites in the peak aged (T6) condition

AlNi intermetallic phase formed increased with increasing weight fraction of Ni particles.

4. SEM-EDAX analysis of composites in the peak aged (T6) condition revealed that the amount of AlNi intermetallic phase formed increased with an increase in weight fraction of Ni particles since the number of heterogeneous nucleation sites were increased. It can be said that AA6061 + 1.5 Wt% Ni composite has higher amount of AlNi intermetallic reinforcements. The increased amount of AlNi intermetallic phase in the composites with increasing weight fraction of Ni particles can be attributed to dissolution of Ni particles in the peak aged (T6) condition. This resulted in higher hardness and more effective grain refinement of composites than the base alloy in the peak aged (T6) condition.
5. Statistical analysis of wear loss and COF revealed that sliding speed shown a higher influence followed by Ni particles weight fraction and load. AA6061 + 1.5 Wt% Ni composite showed the least wear loss and higher COF for all the test conditions compared to other composites and the base alloy.
6. Wear morphology revealed that base alloy and composite samples exhibited adhesive wear mechanism. AA6061 + 1.5 Wt% Ni composite showed better wear resistance than other composites with lesser wear tracks, debris and mild delamination even at sliding speed of 3 m/s. This is due to increased hardness imparted by grain refinement as well as higher amount of AlNi intermetallic phase formation in the AA6061 alloy.

REFERENCES

[1] M. Balakrishnan, I. Dinaharan, K. Kalaiselvan, R. Palanivel, Friction stir processing of Al3Ni intermetallic particulate reinforced cast aluminum matrix composites: Microstructure and tensile properties, J. Mater. Res. Technol. **9**, 4356-4367 (2020). DOI: https://doi.org/110.101610.1016/j.jmrt.2020.02.060

[2] T.P.D. Rajan, R.M. Pillai, B.C. Pai, Functionally graded Al-Al_3Ni in situ intermetallic composites: Fabrication and microstructural characterization, Journal of Alloys and Compounds **453**, L4-L7 (2008). DOI: https://doi.org/10.1016/j.jallcom.2006.11.181

[3] K.S. Mohammad, H.T. Naeem, Effect of milling parameters on the synthesis of Al-Ni intermetallic compound prepared by mechanical alloying. ФИЗИКА МЕТАЛЛОВ И МЕТАЛЛОВЕДЕНИЕ **116**, 908-917(2015). DOI: https://doi.org/10.7868/S0015323015090077

[4] S. Deevi, V. Sikka, Nickel and iron aluminides: an overview on properties, processing, and applications, Intermetallics **4**, 357-375 (1996). DOI: https://doi.org/10.1016/0966-9795(95)00056-9

[5] S. Miura, C. Liu, Effects of aluminum concentration and compact thickness on reaction synthesis ofNi3Al2NiAl alloys, Intermetallics **2**, 297-313 (1994). DOI: https://doi.org/10.1016/0966-9795(94)90016-7

[6] C. Suryanarayana, Mechanical alloying and milling, Progress in Materials Science **46**, 1-184 (2001). DOI: https://doi.org/10.1016/s0079-6425(99)00010-9

[77] H.T. Naeem, K.S. Mohammed, K.R. Ahmad, Azmi Rahmat, The Influence of Nickel and Tin Additives on the Microstructural and Mechanical Properties of Al-Zn-Mg-Cu Alloys, Advances in Materials Science and Engineering, Article ID 686474, 2014. DOI: https://doi.org/10.1155/2014/686474

[8] A.R. Farkoosh, M. Javidani, M. Hoseini, D. Larouche, M. Pekguleryuz, Phase formation in as-solidified and heat treated Al-Si-Cu-Mg-Ni alloys: thermodynamic assessment and experimental investigation for alloy design, Journal of Alloys and Compounds **551**, 596-606 (2013). DOI: https://doi.org/10.1016/j.jallcom.2012.10.182

[9] R.S. Mishra, Z.Y. Ma, I. Charit, and Friction stir processing: a novel technique for fabrication of surface composite, Mater. Sci. Eng. A. **341**, 307-310 (2003). DOI: https://doi.org/10.1016/s0921-5093 (02)00199-5

[10] Y. Morisada, H. Fujii, T. Nagaoka, K. Nogi, M. Fukusumi, Fullerene/A5083 composites fabricated by material flow during friction stir processing, Compos. Part A **38**, 2097-2101 (2007). DOI: https://doi.org/10.1016/j.compositesa.2007.07.004

[11] Y. Morisada, H. Fujii, T. Nagaoka, M. Fukusumi, Effect of friction stir processing on the microstructure and hardness of an aluminum-zinc-magnesium-copper alloy with nickel additives, Mater. Sci. Eng. A **419**, 344-348 (2006). DOI: https://doi.org/10.7868/s0015323015100058

[12] M. Dixit, J.W. Newkir, R.S. Mishra, Properties of friction stir-processed Al 1100-NiTi composite, Scripta Mater. **56**, 541-544 (2007). DOI: https://doi.org/10.1016/j.scriptamat.2006.11.006

[13] W.B. Li, Q.L. Pan, Y.P. Xiao, Y.B. He, X.Y. Liu, Microstructural evolution of ultra-high strength Al-Zn-Cu-Mg-Zr alloy containing Sc during homogenization, Transactions of Nonferrous Metals Society of China **21** (10), 2127-2133 (2011). DOI: https://doi.org/10.1016/s1003-6326(11)60984-9

[14] G.S. Peng, K.H. Chen, S.Y. Chen, H.C. Fang, Influence of dual retrogression and re-aging temper on microstructure, strength and exfoliation corrosion behavior of Al-Zn-Mg-Cu alloy, Transactions of Nonferrous Metals Society of China **22** (4), 803-809 (2012). DOI: https://doi.org/10.1016/s1003-6326(11)61248-x

[15] S. Çam, V. Demir, D. Özyürek, Wear Behaviour of A356/$TiAl_3$ *in Situ* Composites Produced by Mechanical Alloying, Metals. 6 (2), 34 (2016). DOI: https://doi.org/10.3390/met6020034

[16] J. Qian, J. Li, J. Xiong, F. Zhang, X. Lin, In situ synthesizing Al3Ni for fabrication of intermetallic-reinforced aluminum alloy composites by friction stir processing, Materials Science and Engineering A **550**, 279-285 (2012). DOI: https://doi.org/10.1016/j.msea.2012.04.070

[17] O.P. Gbenebor, M. Abdulwahab, O.S.I. Fayomi, Influence of inoculant addition and cooling medium on the mechanical properties of AA6063-typeAl-Mg-Si alloy, Chalcogenide Letters **9** (5), 201-211 (2012).

[18] R. Nadella, D.G. Eskin, Q. Du, L. Katgerman, Macrosegregation in direct-chill casting of aluminium alloys, Progress in Materials Science **53** (3), 421-480 (2008).
DOI: https://doi.org/10.1016/j.pmatsci.2007.10.001

[19] G. Liu, N. Zhao, C. Shi, E. Liu, F. He, L. Ma, Q. Li, J. Li, C. He, In-situ synthesis of graphene decorated with nickel nanoparticles for fabricating reinforced 6061Almatrix composites, Material Science & Engineering A **699**, 185-193 (2017).
DOI: https://doi.org/10.1016/j.msea.2017.05.084

[20] B.S.B. Reddy, K. Rajasekhar, M. Venu, J.J.S. Dilip, S. Das, K. Das, Mechanicalactivation assisted solid-state combustion synthesis of in situ aluminum matrix hybrid (Al_3Ni/Al_2O_3) nanocomposite, Journal of Alloys and Compounds **465**, 97-105 (2008).
DOI: https://doi.org/10.1016/j.jallcom.2007.10.098

[21] A.R. Najarian, R. Emadi, M. Hamzeh, Fabrication of as-cast Al matrix composite reinforced by Al2O3/Al3Ni hybrid particles via in-situ reaction and evaluation of its mechanical properties, Materials Science & Engineering B **231**, 57-65 (2018).
DOI: https://doi.org/10.1016/j.mseb.2018.09.002

[22] R. Ramesh, S. Suresh Kumar, S. Gowrishankar, Production and characterization of aluminium metal matrix composite reinforced with Al3Ni by stir and squeeze casting, Applied Mechanics and Materials **766-767**, 315-319 (2015).
DOI: https://doi.org/10.4028/www.scientific.net/AMM.766-767.315

[23] T. Satish kumar, S. Shalini, K. Krishna Kumar, Synthesis and characterization of al-zn-mg alloy / zircon sand reinforced composites, Arch. Metall. Mater. **63** (2), 689-695(2018).
DOI: https://doi.org/10.24425/122395

[24] R. Srinivasan, H.K. Shivananad, Studies on Tribological characterization of Carbon Nanotube reinforced with 6061 Aluminium Alloy Metal Matrix Composites coated with Nickel, International Journal of Applied Engineering Research **14**, 3721-3729 (2019).

[25] M. Zadali, M. Kotiyani, K. Ranjbar, Wear and corrosion of in-situ formed Al_3Zr aluminide reinforced Al3003 surface composite, IJMR **110**, 874-884 (2019).
DOI: https://doi.org/10.3139/146.111819

[26] N. Radhika, R. Subramanian, Effect of ageing time on mechanical and tribological behaviour of Al hybrid composite, IJMR **105**, 875-882 (2014).
DOI: https://doi.org/10.3139/146.111098